Supporting information

Electrokinetic control of bacterial deposition and transport

Jinyi Qin[1], Xiaohui Sun[2], Yang Liu[2], Tom Berthold[1], Hauke Harms[1], Lukas Y. Wick[1,2]*

[1] *UFZ - Helmholtz Centre for Environmental Research, Department of Environmental Microbiology, 04318 Leipzig, Germany*

[2] *University of Alberta, Department of Civil and Environmental Engineering, 3-133 Markin/CNRL Natural Resources Engineering Facility, Edmonton, AB, T6G 2W2, Canada*

The revised supporting information contains 17 Pages, 8 Figures and 2 Tables.

* Corresponding author: Mailing address: Helmholtz Centre for Environmental Research - UFZ. Department of Environmental Microbiology; Permoserstrasse 15; 04318 Leipzig, Germany. phone: +49 341 235 1316, fax: +49 341 235 1351, e-mail: lukas.wick@ufz.de.

Theory and Calculations

Calculation of the collision efficiency (α_t)

The collision efficiency (α_t) of bacteria was calculated applying the clean-bed filtration theory [1] (eq. 2). The α_t of bacteria is defined as the ratio of the rate of attachment (n_t) to the rate of bacterial transport to the surfaces(n_{trans}). Therefore, α_t represents the relative affinity of bacteria for the packing material and $\alpha_{t,0}$ represents the initial collision efficiency. DC free control runs ($\alpha_{t,\text{control}}$) and runs in the presence of an electric field ($\alpha_{t,DC}$) are subject to the different percolation regimes and were compared with the percentage change was

$$Percentage\ change = \frac{\alpha_{t,control} - \alpha_{t,DC}}{\alpha_{t,0}} \times 100 \quad (1)$$

Values of n_{trans} were calculated taking into account the contributions of convection, diffusion, van der Waals attraction, and sedimentation [2]. For the calculations, we assumed spheres of identical size glass beads (diameter: 0.1 mm) in their closest packing, and identical effective bacterial radius (1 μm) of the bacteria. Values of n_t were calculated from C/C_0 values obtained in column experiments.

$$C = C_0 \exp\left(-\frac{3(1-\varepsilon)}{4a_s} n_{trans} \alpha_t L\right) \quad (2)$$

where C is the effluent cell concentration, C_0 the influent cell concentration, ε the porosity of the packed bed, a_s the radius of the glass beads, L the length of the column, and n_t the transport of bacteria from the solution to the glass surface in the whole experimental time. n_{trans} was approximated by applying the solution to convection-diffusion equation (eq. 3):

$$n_{trans} = A_s \frac{A_{132}}{9\pi\eta a_b{}^2 \upsilon}^{0.125} \frac{a_b}{a_s}^{1.875} + 0.00338 A_s \frac{2a_b{}^2(\rho_b - \rho_l)g}{9\eta\upsilon}^{1.2} \frac{a_b}{a_s}^{-0.4} + 4A_s{}^{0.33} \frac{12\upsilon a_s \pi\eta a_b}{kt}^{-0.67} \quad (3)$$

$$A_s = \frac{2(1-(1-\varepsilon)^{1.67})}{2-3(1-\varepsilon)+3(1-\varepsilon)^{1.67}-2(1-\varepsilon)^2} \quad (4)$$

with ε being the porosity of column (0.41), a_b and a_s are the radii of bacteria ($a_b = 10^{-6}$ m) and the glass beads ($a_s = 5 \times 10^{-5}$ m), respectively, η and ρ_l are the absolute viscosity (η = 3.19 kg m^{-1} h^{-1}) and density of buffer solution (ρ =*1000 kg* m^3), v is the approach velocity (1.1×10^{-4}

m s^{-1}), g is the gravitational acceleration (9.81 ms^{-2}) , k is the Bolzmann constant (1.38 × 10^{-23} J K^{-1}), t is the room temperature of 293K. ρ_b is the density of the bacteria solution , (ρ_b = *1090 kg* m^3) and A_{132} is the Hamaker constant [2] as described by eq. 5 [3]

$$A_{132} = (\sqrt{A_{11}} - \sqrt{A_{33}})(\sqrt{A_{22}} - \sqrt{A_{33}}) \quad (5)$$

Here, A_{ii} denotes the individual Hamaker constant of bacteria (A_{11}), glass (A_{22},) and water (A_{33}), respectively. A_{33} was taken from literature [4] whereas A_{11} and A_{22} were obtained by eq. 6 [5].

$$A_{ii} = 6\pi l_0^{\,2} \gamma_i^{LW} \quad (6)$$

According to Fowkes [5], the value of $6\pi l_0^2$ equals 1.44 × 10^{-18} m^2, with l_0 being the minimum distance between the outermost cell surface and the glass bead (0.157 nm) [6]. Thus, the individual and effective Hamaker constants in media were assessed in Table S2. Derick et al. have reported that Hamaker constant (A_{132}) values range from 0.28 to 3.46 ×10^{-21} J for quartz surface [6]. For the interaction of cellulose with SiO_2, the Hamaker constant was in the range of 0.32 - 0.38[7]. The value of the Hamaker constant used in our study is consistent with these values.

Calculations of surface coverage and the fraction of bacteria retained

Assuming that the entire glass surface allows for irreversible adhesion, the fraction of bacterial coverage on the surface can be described by eq. 7:

$$\theta = \frac{N_b \pi a_b^{\,2}}{N_s 4\pi a_s^{\,2}} \quad (7)$$

where N_s and N_b are the numbers of collectors and bacteria in the column and a_b and a_s the radii of bacteria and the collectors, respectively [8].

The fraction of bacteria retained in the column, R is calculated by eq. 8:

$$R = \int (1 - \frac{C}{C_0}) \cdot dV \quad (8)$$

where C and C_0 are the effluent and influent cell concentrations of the column, and V the flow of the cell suspension (V = 19 ml h^{-1}) through the column [9, 10].

Calculation of XDLVO interaction energy of bacterial adhesion

According to the extended DLVO theory [11], the XDLVO interaction energy of bacterial adhesion (G_{XDLVO}) is composed of the acid-base (G_{AB}) interaction energy, the electrostatic repulsion (G_{EDL}), and the Lifshitz-van der Waals (G_{LW}) energy (eq. 9) [11]:

$$G_{XDLVO} = G_{AB} + G_{EDL} + G_{LW} \quad (9)$$

Acid-base interaction energy (G_{AB}). The acid-base interaction energy (G_{AB}) depends on the Gibbs free energy of the bacteria and the glass as given by eq. 10, in which a_b is the radius of bacteria (1 μm), and h is the separation distance between the bacterium and the surface. The λ is the characteristic decay length of AB interaction in water (estimated 0.6nm) [11].

$$G_{AB} = 2\pi a_b \Delta G^{AB} \lambda \exp(\frac{l_0 - h}{\lambda}) \quad (10)$$

ΔG^{AB} is the acid-base component of the free energy interaction at contact given by eq. 11 [12, 13]

$$\Delta G^{AB} = 2\begin{bmatrix} (\sqrt{\gamma_b^+} - \sqrt{\gamma_s^+})(\sqrt{\gamma_b^-} - \sqrt{\gamma_s^-}) - (\sqrt{\gamma_b^+} - \sqrt{\gamma_l^+})(\sqrt{\gamma_b^-} - \sqrt{\gamma_l^-}) \\ -(\sqrt{\gamma_s^+} - \sqrt{\gamma_l^+})(\sqrt{\gamma_s^-} - \sqrt{\gamma_l^-}) \end{bmatrix} \quad (11)$$

The surface Gibbs free energies of bacteria γ_b and the glass surface γ_s (mJ m^{-2}) were calculated based on measured contact angles (θ) of microbial lawns, membrane filters and glass surfaces using water, formamide and methylene iodide as liquids using the Young equation according to eq. 12:

$$Cos(\theta) = -1 + 2\frac{\sqrt{\gamma_b^{LW}\gamma_l^{LW}}}{\gamma_l^{total}} + 2\frac{\sqrt{\gamma_b^+\gamma_l^-}}{\gamma_l^{total}} + 2\frac{\sqrt{\gamma_b^-\gamma_l^+}}{\gamma_l^{total}} \quad (12)$$

The total surface Gibbs free energies (γ^{total}) thereby were separated in a Lifshitz-van der Waals (γ^{LW}) and an acid-base component (γ^{AB}) (eq. 13) with γ^+ and γ^- as the electron acceptor and the electron donor components of acid-base surface energy (eqs. 13 & 14).

$$\gamma^{total} = \gamma^{AB} + \gamma^{LW} \quad (13)$$

$$\gamma_i^{AB} = 2\sqrt{\gamma_i^+\gamma_i^-} \quad (14)$$

Using literature data [14] of γ, γ^{LW}, γ^{+}, γ^{-} values for water, formamide and methyleneiodide, the parameters γ_b, γ_b^{LW}, γ_b^{+}, γ_b^{-} of bacteria were calculated as proposed by van Oss et al[15], and the data from literature taken for assessing the free energy of the glass surface [16].

Electrostatic repulsion energy, (G_{EDL}). The electrostatic repulsion energy between bacteria and the glass surface was calculated by eq. 15 [11]:

$$G_{EDL} = \pi\varepsilon_0\varepsilon_r a_b \left\{ 2\xi_b\xi_s \ln\left[\frac{1+\exp(-\kappa h)}{1-\exp(-\kappa h)}\right] + (\xi_b^{\,2} + \xi_s^{\,2}) \ln\left[1-\exp(-2\kappa h)\right] \right\} \quad (15)$$

where κ^{-1} is the thickness of electrical double layer (EDL, nm) as calculated by the Guoy-Chapman theory with C and z being the molar bulk concentration and the charge number of the electrolytes[14] (eq. 16).

$$\kappa^{-1} = \left[3.29 z C^{1/2}\right]^{-1} \quad (16)$$

For a 10 mM and a 100 mM buffer solution, a $\kappa^{-1}$of 2.15 nm (10 mM buffer) and κ^{-1} of 0.65 nm (100 mM buffer) were calculated.

Lifshitz-van der Waals interaction energy (G_{LW}). With given values of the effective Hamaker constant, the Lifshitz-van der Waals interaction energy can be calculated by eq. 17 [13-15, 17]

$$G_{LW} = -\frac{A_{132}}{6}\left[\frac{2a_b(h+a_b)}{h(h+2a_b)} - \ln\left(\frac{h+2a_b}{h}\right)\right] \quad (17)$$

Tables

Table S1. Overview of the surface free energy (γ) and the contact angles of water θ_w, methylene iodide θ_m and formamide θ_f of glass and bacterial lawns of *P. fluorescens* Lp6a.

	Contact angle (Θ)			Surface free energy γ (mJ m^{-2}) [1]				
	Θ_w	Θ_f	Θ_m	γ^-	γ^+	γ^{AB}	γ^{LW}	γ^{Tot}
Water				25.5	25.5	51	21.8	72.8
Formamide				39.6	2.3	19	39	58
Methyleneiodide				<0.1	<0.1	≈0	50.8	50.8
***P. fluorescens* Lp6a**	16.1	35.1	54.4	61.7	0.9	14.8	31.7	46.5
Glass	23	16	53	50.8	3	24.8	32.4	57.2

[1] Data for water, formamide, methyleneiodide and glass taken from: [6, 18].

Table S2. Overview of the individual Hamaker constants (A_{ii}) of the bacteria (A_{11}), glass (A_{22},) and water (A_{33}), respectively. The calculated effective Hamaker constant is denoted by A_{123}.

	A_{11}	A_{22}	A_{33}	A_{132}
***P. fluorescens* Lp6a (×10^{-21} J)**	**45.6**	**46.7**	**37**	**0.5**

References

1. Velasco-Casal, P.; Wick, L. Y.; Ortega-Calvo, J. J., Chemoeffectors decrease the deposition of chemotactic bacteria during transport in porous media. *Environ Sci Technol* **2008,** *42*, (4), 1131-1137.
2. Martin, R. E.; Bouwer, E. J.; Hanna, L. M., Application of Clean-Bed Filtration Theory to Bacterial Deposition in Porous-Media. *Environ Sci Technol* **1992,** *26*, (5), 1053-1058.
3. Van Oss, C. J.; Good, R. J.; Chaudhury, M. K., The Role of van der Waals Forces and Hydrogen Bonds in "Hydrophobic Interactions" between Biopolymers and Low Energy Surfaces. *J Colloid Interface Sci* **1985,** *111*, (2).
4. Vilinska, A.; Rao, K. H., Surface thermodynamics and extended DLVO theory of *Leptospirillum ferrooxidans* cells' adhesion on sulfide minerals. *Miner Metall Proc* **2011,** *28*, (3), 151-158.
5. Fowkes, F. M., Attractive Forces at Interfaces. *Ind Eng Chem* **1964,** *56*, (12), 40-&.
6. Brown, D. G.; Jaffe, P. R., Effects of nonionic surfactants on the cell surface hydrophobicity and apparent hamaker constant of a *Sphingomonas sp*. *Environ Sci Technol* **2006,** *40*, (1), 195-201.
7. Bergström, L.; Stemme, S.; Dahlfors, T.; Arwin, H.; Ödberg, L., Spectroscopic Ellipsometry Characterisation and Estimation of the Hamaker Constant of Cellulose. *Cellulose* **1999,** *6*, (1), 1-13.
8. Johnson, W. P.; Blue, K. A.; Logan, B. E.; Arnold, R. G., Modeling Bacterial Detachment during Transport through Porous-Media as a Residence-Time-Dependent Process. *Water Resour Res* **1995,** *31*, (11), 2649-2658.
9. Jewett, D. G.; Logan, B. E.; Arnold, R. G.; Bales, R. C., Transport of *Pseudomonas fluorescens* strain P17 through quartz sand columns as a function of water content. *J Contam Hydrol* **1999,** *36*, (1-2), 73-89.
10. Rijnaarts, H. H. M.; Norde, W., Reversibility and mechanism of bacterial adhesion. *Colloids Surf B Biointerfaces* **1995,** *4*, 5-22.
11. Boks, N. P.; Norde, W.; van der Mei, H. C.; Busscher, H. J., Forces involved in bacterial adhesion to hydrophilic and hydrophobic surfaces. *Microbiol-Sgm* **2008,** *154*, 3122-3133.
12. Van Oss, C. J.; Docoslis, A.; Wu, W.; Giese, R. F., Influence of macroscopic and microscopic interactions on kinetic rate constants - I. Role of the extended DLVO theory in determining the kinetic adsorption constant of proteins in aqueous media, using von Smoluchowski's approach. *Colloids Surf B Biointerfaces* **1999,** *14*, (1-4), 99-104.
13. Vanoss, C. J.; Giese, R. F.; Costanzo, P. M., DLVO and Non-DLVO interactions in Hectorite. *Clay Clay Miner* **1990,** *38*, (2), 151-159.
14. Sharma, P. K.; Rao, K. H., Adhesion of *Paenibacillus polymyxa* on chalcopyrite and pyrite: surface thermodynamics and extended DLVO theory. *Colloids Surf B Biointerfaces* **2003,** *29*, (1), 21-38.
15. Van Oss, C. J.; Chaudhury, M. K.; Good, R. J., Interfacial Lifshitz-van der Waals and polar interactions in macroscopic systems. *Chem Rev* **1988,** *88*, (6), 927-941.
16. Meylheuc, T.; Bellon-Fontaine, M. N., *Pseudomonas fluorescens* - prodution of biosurfactants and impact of their bioadhesive behaviour. **2003**.
17. Chia, T. W. R.; Nguyen, V. T.; McMeekin, T.; Fegan, N.; Dykes, G. A., Stochasticity of Bacterial Attachment and Its Predictability by the Extended Derjaguin-Landau-Verwey-Overbeek Theory. *Appl Environ Microb* **2011,** *77*, (11), 3757-3764.
18. Bolina, A. S.; Wolff, A. J.; Brown, W. A., Reflection absorption infrared spectroscopy and temperature-programmed desorption studies of the adsorption and desorption of amorphous and crystalline water on a graphite surface. *J Phys Chem B* **2005,** *109*, (35), 16836-45.

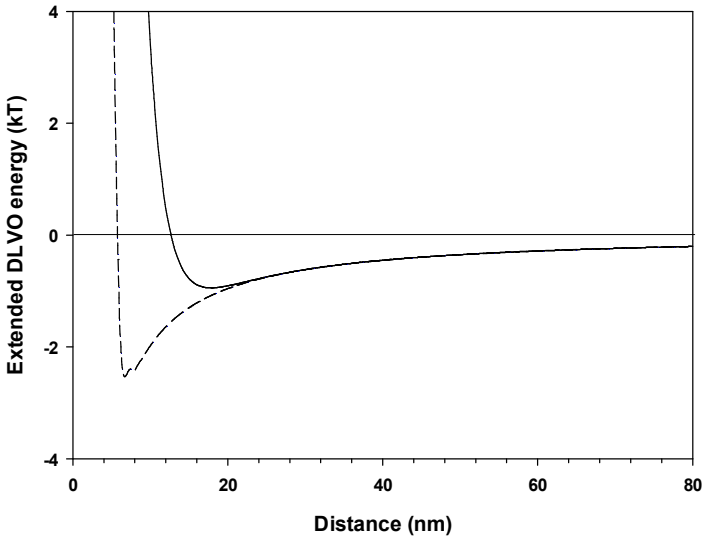

158

159

160 **Figure S1.** Profile of the extended XDLVO interaction energy (1 kT = 4.0 × 10^{-21} J) as a
161 function of the distance for *P. fluorescens* Lp6a cell on glass surface in 10 mM (solid line)
162 and 100 mM (dashed line) buffer solution.

163

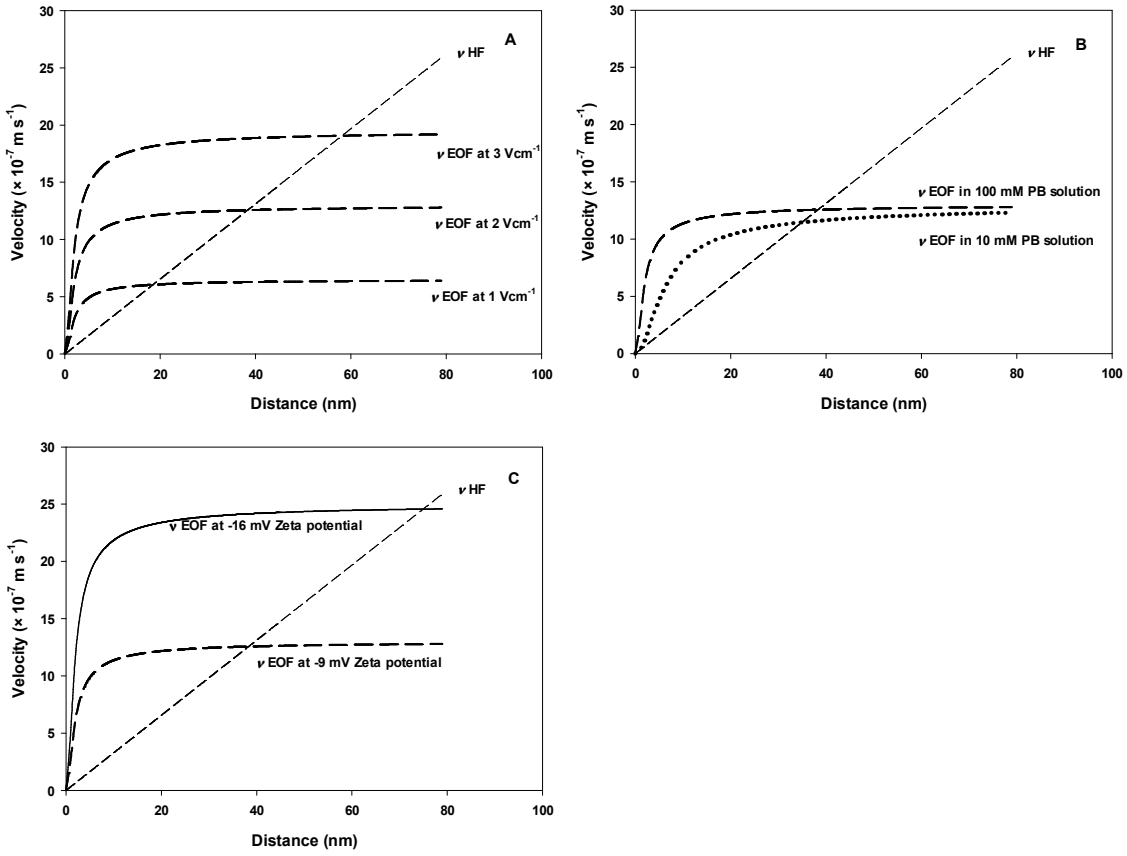

164

165

166

167 **Figure S2.** Calculated velocity profiles of the electroosmotic (υ_{EOF}; dashed lines) and the
168 hydraulic flow (υ_{HF}; fine dashed line) as a function of the distance to a glass surface at
169 varying electric field strengths, ionic strengths and zeta potentials of the glass surfaces. Figure
170 S2A: ζ = -9 mV; 100 mM buffer, X = 1, 2, or 3 V cm^{-1}; Figure S2B: ζ = -9 mV; 10 and 100
171 mM buffer, X = 2 V cm^{-1}; Figure S2C: ζ = -9 and -16 mV; 100 mM buffer, X = 2 V cm^{-1}.

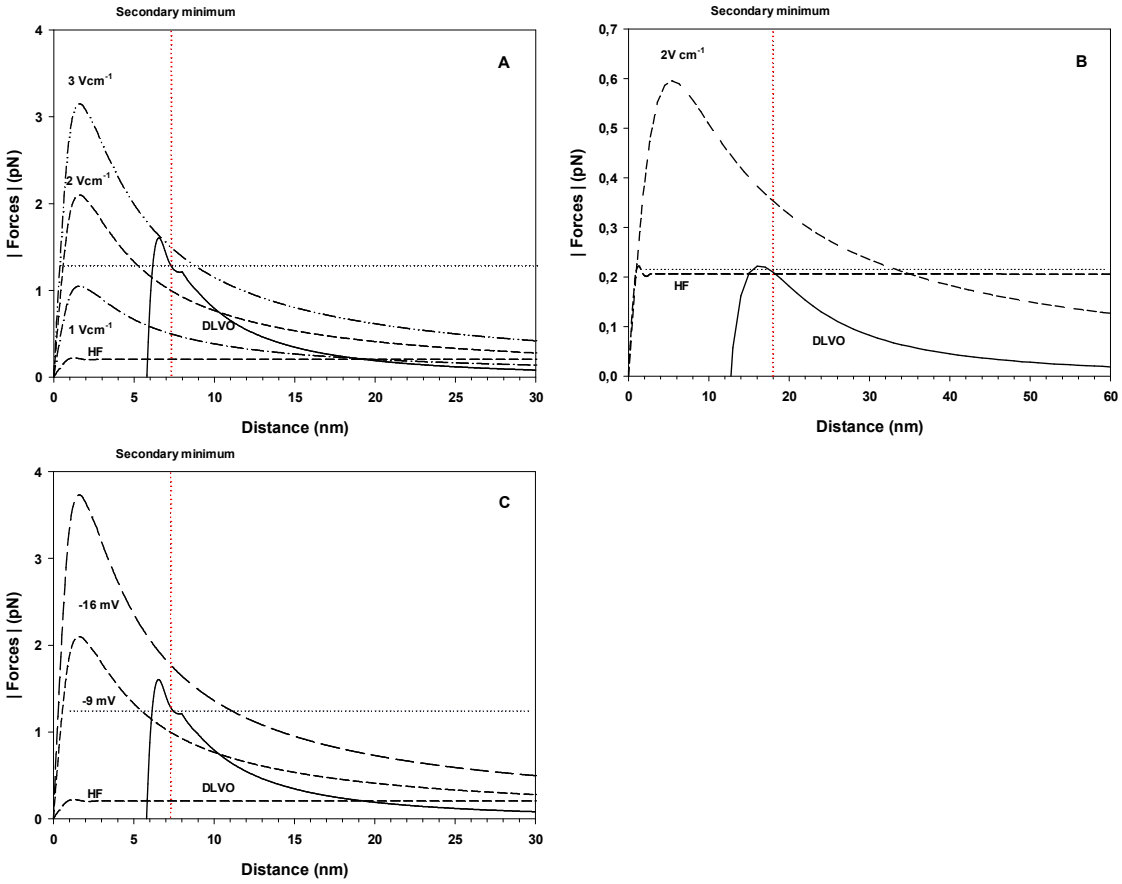

172

173

174 **Figure S3.** Calculated profiles of the shear forces induced by the electroosmotic (big dashed
175 lines) and the hydraulic flow (short dashed line) acting on *P. fluorescens* Lp6a cell. Please
176 note that the change of ζ from -9 mV to -16 mV did not result in printable (i.e. minimal)
177 changes of the XDLVO force and hence is not further detailed in the graph. The solid line
178 represents the calculated profile of the absolute value of the calculated XDLVO maximum
179 attractive force acting on a *P. fluorescens* Lp6a cell. Dotted vertical and horizontal lines
180 represent the calculated distance of the secondary minimum and the absolute value of the
181 maximum XDLVO attractive force, respectively. Figure S3A: ζ = -9 mV; 100 mM buffer, X =
182 1, 2, or 3 V cm^{-1}; Figure S3B: ζ = -9 mV; 10 mM buffer, X = 2 V cm^{-1}; Figure S3C: ζ = -9 and
183 -16 mV; 100 mM buffer, X = 2 V cm^{-1}.

184

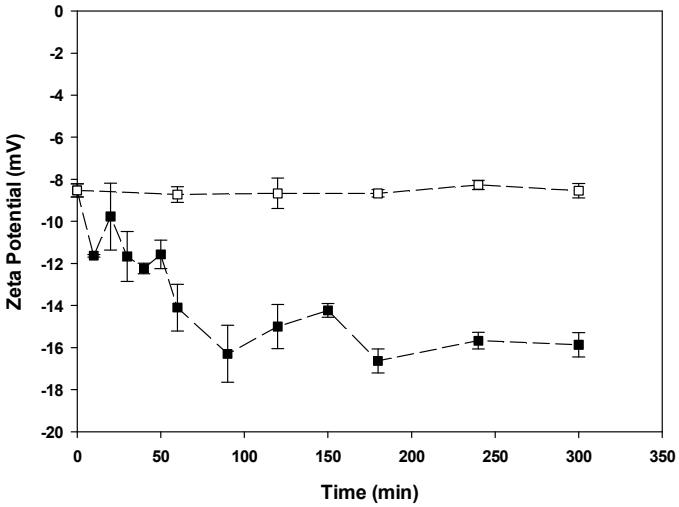

185

186

187 **Figure S4.** Effect of time (300 minutes) on the zeta potential of glass beads (squares) during
188 exposure of to a bacterial suspension (OD_{578} = 0.3; filled squares) and a cell free control
189 (open squares).

190

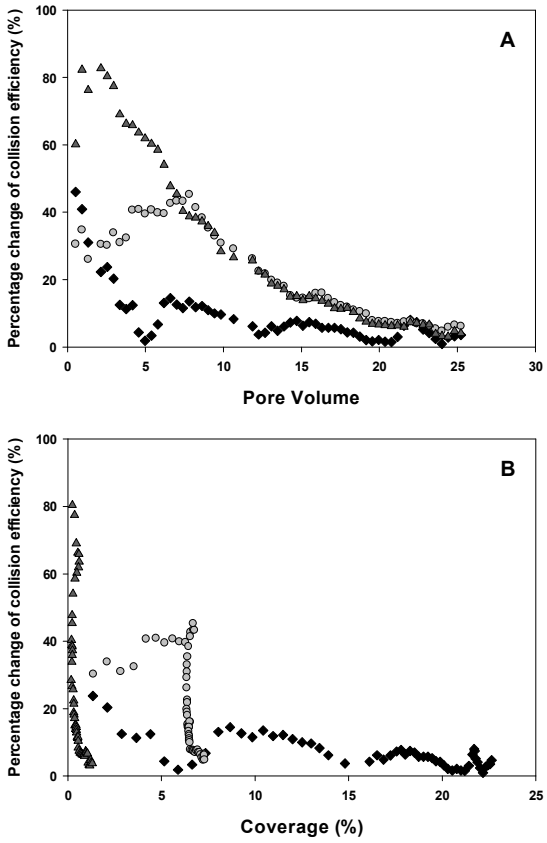

191

192

193 **Figure S5.** The reduction of Collision efficiency was changing as a function of the pore
194 volume (Fig. S5A) and bacterial coverage (Fig. S5B): Triangles refer to $X = 3$ V cm^{-1}, circles
195 to $X = 2$ V cm^{-1} and diamonds to $X = 1$ V cm^{-1}.

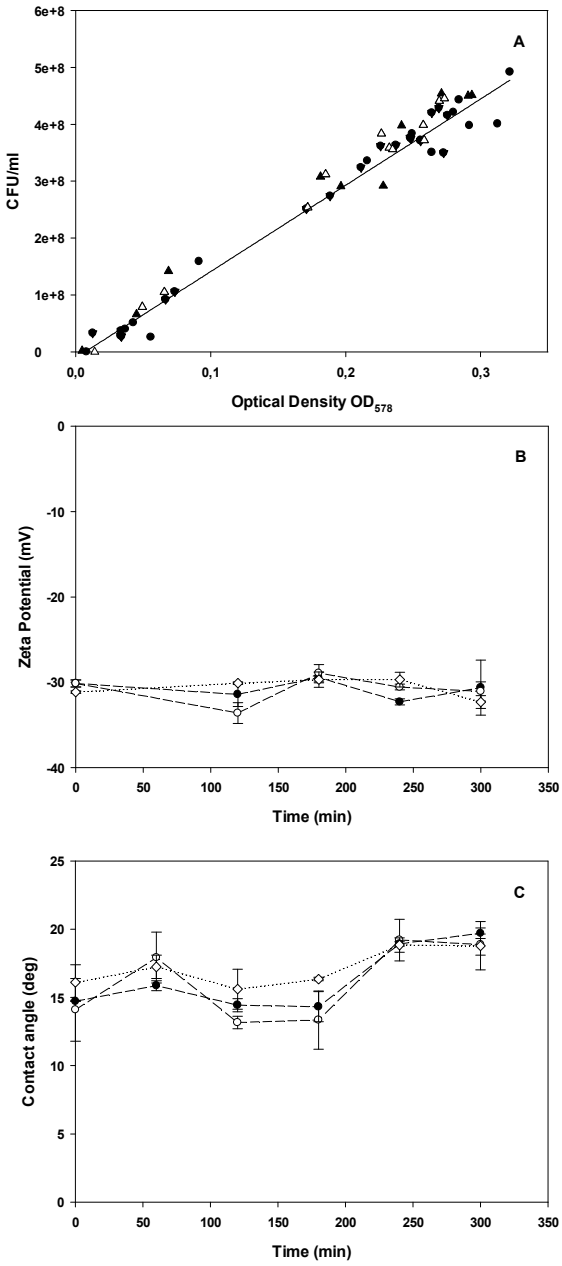

196

197

198 **Figure S6.** Effect of the electrokinetic treatment on the viability, zeta potential and water
199 contact angle of *P. fluorescens* Lp6a cells at the outflow of percolation columns filled with
200 glass beads the absence (empty symbols) and presence (filled symbols) of an DC electric field
201 of X = 1 V cm^{-1} (filled triangles) and X = 2 V cm^{-1} (filled circles) over time. Figure S5A:
202 Comparison of the optical density (578 nm) and the colony forming units on LB agar plates
203 (cfu) of strain Lp6a in the outflow of the columns; Figure S5B: Zeta potential of outflow cell
204 vs time; dotted line represents the zeta potential of the inflowing cells; Figure S5C: Water
205 contact angle of outflowing cells over time; dotted line represents the water contact angle of
206 the inflowing cells.

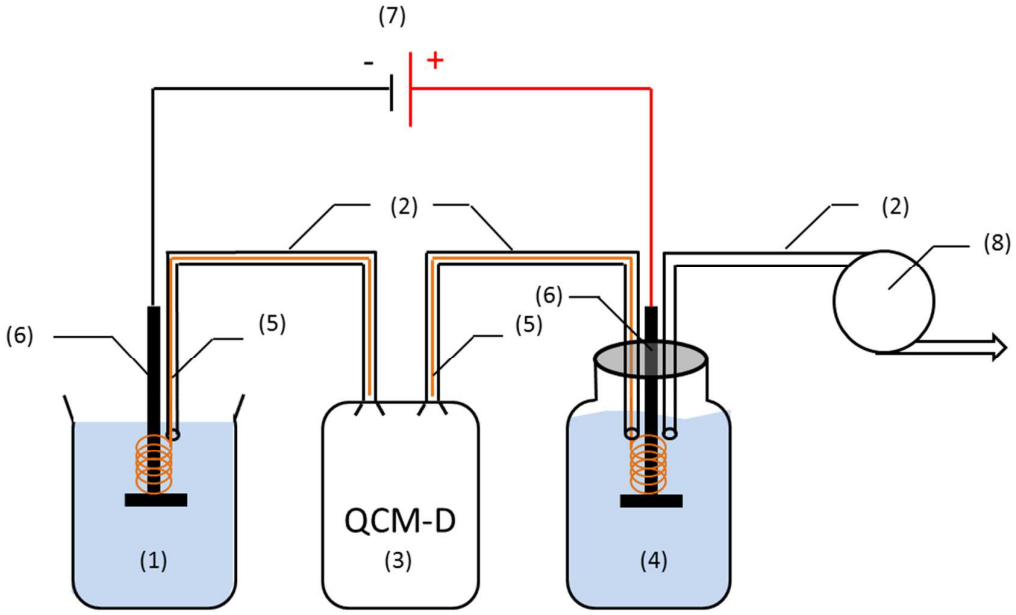

Figure S7. Schematic graph of the quartz crystal microbalance with dissipation measurement (QCM-D) under applied DC electric field: By using a peristaltic pump (8) a bacterial suspension was withdrawn by underpressure from a reservoir (1) and pumped through the QCM-D sensor chamber (3) into a recipient container (4). Disk-shaped Ti/Li electrodes (6) were connected to two copper wires (5) that extended electrodes through the Teflon tubing (2) to the QCM chamber. A power pack (7) was used to apply a constant DC electric field as indicated in the figure.

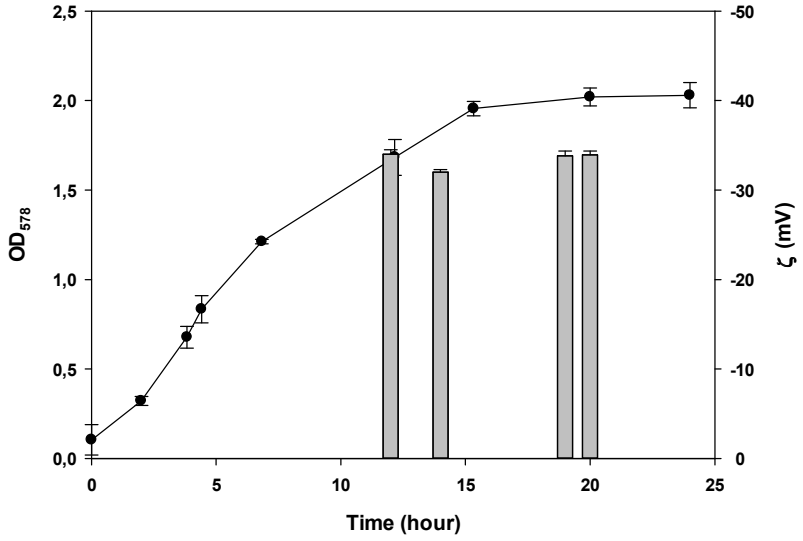

Figure S8. The *LP6a* bacteria growths curve (left) and measured zeta potential ζ (bar, right) as function of time

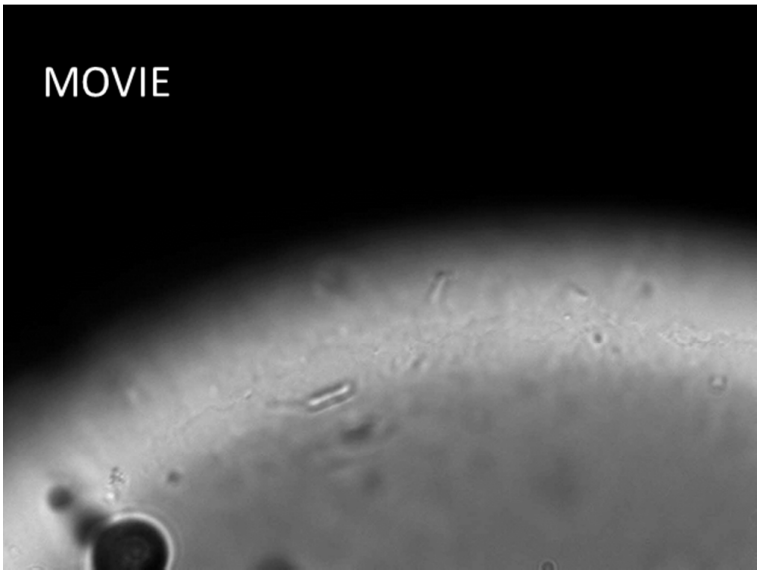

Movie 1. A 30 s time-lapse video showing the movement of *P. fluorescens* Lp6a cells attached to glass beads, in the presence and absence of a 2 Vcm^{-1} electric field can be found at http://pubs.acs.org. The surface of the glass beads is visible at the bottom of the picture. The rod-shaped bacteria attached to the surface, is highlighted as red torus. Initially, no electrical field is applied to the solution. After 10 sec, the electric field was switched on and negatively charged cell is attracted by the anode. Meanwhile, the induced the EOF moves in the opposite direction, from anode to the cathode. Prior to the microscopy experiment, a pre-culture of the bacteria was grown to an OD_{578} = 0.3 and used to inoculate a culture with sterile glass beads (0.1 – 0.25 mm diameter) in mineral media with 1 gL^{-1} glucose in a flask. This culture was stationary incubated for 3 days at room temperature to allow cell attachment on the glass surface. The glass beads were subsequently picked out cautiously and transferred to a glass bottom dish (50mm μ-Dish ,Ibidi GmBH, Munich, Germany) using 1 mL pipette. Glass beads were rinsed with 3 mL potassium phosphate buffer for three times to wash away non-attached cells and gently resuspended in buffer solution. The anode and cathode grid electrodes were applied on the right and left side of petri dish respectively. Attached bacterial cells were visualized by light microscopy on an Axio Observer.Z1 inverted microscope, using a Plan-Apochromat 100x/1.4 objective (both Carl Zeiss AG, Oberkochen, Germany) and a frame rate of 5 fps.